


Article

Physical Properties, Chemical Structure, and Microstructure of Thermoplastic Polyurethane Recycled Material-Modified Asphalt

Peng Yang ^{1,2,*} , Peiliang Cong ³, Hongjie Hao ³ and Pengfei Xiong ⁴¹ School of Intelligent Transportation and Engineering (School of Future Transportation), Guangzhou Maritime University, Guangzhou 510725, China² Guangdong Key Laboratory of Materials and Equipment in Harsh Marine Environment, Guangzhou Maritime University, Guangzhou 510725, China³ School of Materials Science and Engineering, Chang'an University, Xi'an 710064, China; congpl@chd.edu.cn (P.C.); cpl9903@163.com (H.H.)⁴ Guangdong Communication Planning & Design Institute Group Co., Ltd., Guangzhou 510440, China; 19860209093@163.com

* Correspondence: yangpeng1209@126.com

Abstract: Firstly, thermoplastic polyurethane recycled material (TPRM) particles were used to prepare modified asphalt. Then, the modified asphalt's physical properties were investigated. The results show that the TPRM particles improved its high-temperature performance, low-temperature crack resistance, and shear behavior due to its increased cohesion and low-temperature fracture energy levels. Thermal susceptibility was affected by the degree of swelling and dissolution of the TPRM particles, the composition of the asphalt, and the interface effect between the asphalt molecules and both the regular and slender-irregular TPRM particles. The TPRM particles swelled and dissolved after absorbing the light components of asphalt. Changes in the shearing temperature and time made the TPRM particles swell and dissolve more than changes in the activation temperature and time. An increase in the shearing/activation temperature and time increased the hydrogen bond content in the modified asphalt due to the rearrangement of the polyurethane's molecular structure and the hydrogen bonds formed by the asphaltene and polyurethane molecules. Slender-irregular TPRM and "sea-island" and hilly and gulley structures were found in the modified asphalt matrix.

Keywords: thermoplastic polyurethane recycled material; modified asphalt; physical properties; chemical structure; microstructure



Academic Editor: Antonio Caggiano

Received: 22 December 2024

Revised: 13 January 2025

Accepted: 14 January 2025

Published: 18 January 2025

Citation: Yang, P.; Cong, P.; Hao, H.; Xiong, P. Physical Properties, Chemical Structure, and Microstructure of Thermoplastic Polyurethane Recycled Material-Modified Asphalt. *Buildings* **2025**, *15*, 281. <https://doi.org/10.3390/buildings15020281>

Correction Statement: This article has been republished with a minor change. The change does not affect the scientific content of the article and further details are available within the backmatter of the website version of this article.

Copyright: © 2025 by the authors. Licensee MDPI, Basel, Switzerland. This article is an open access article distributed under the terms and conditions of the Creative Commons Attribution (CC BY) license (<https://creativecommons.org/licenses/by/4.0/>).

1. Introduction

Asphalt is the byproduct of the petroleum industry and has complex compositions. In the colloid theory, asphalt is divided into four compositions: saturated fractions, aromatic fractions, resin, and asphaltene. Currently, high-grade pavement plays an important role in the development of the national economy, and most pavements are made of asphalt. Due to the influences of temperature, humidity, and moisture, asphalt pavements age quickly and their composition changes. As a result, the content of light components in asphalt decreases, it becomes harder, and it can no longer be cemented or resist wear. This results in cracking, pitting, and other issues, which severely shorten the service life of the pavement [1–3].

At present, in engineering, polymer-modified asphalt is generally used. The polymer modifiers commonly used are styrene butadiene styrene block (SBS) and ethylene-vinyl acetate (EVA) copolymers, styrene butadiene (SBR) and crumb rubber (CR), and polyethylene (PE). Polymer-modified asphalt is usually obtained through physical modification,

and its performance is highly dependent on which polymer is used. After modification, the high-temperature performance and low-temperature crack resistance of asphalt are improved to a certain extent. This can prolong the service life of asphalt pavements, lower infrastructure construction costs, and promote the development of the national economy [4–6]. In addition, some researchers have tried to use polyurethane prepolymer to prepare modified asphalt. Sun et al. used polyurethane prepolymers as an additive to prepare modified asphalt and a mixture. They found that the modified asphalt had excellent high-temperature stability and low-temperature crack resistance, and the mixture was very water-stable [7]. Jin et al. investigated the properties of polyurethane prepolymer and rock asphalt-modified asphalt. The results show that the unsaturated bond in the polyurethane prepolymer crosslinked with an S-S bond in base asphalt improved its low-temperature crack resistance [8]. Xia et al. prepared castor oil–polyurethane prepolymer polyurethane (C-PU)-modified asphalt. The resistance to deformation of this modified asphalt improved with an increasing C-PU content. This is due to the reaction of –NCO with water and active hydrogen in asphalt [9]. Jia et al. used synthetic thermoplastic polyurethane as an additive to improve the low-temperature crack resistance of organic montmorillonite-modified asphalt. This modified asphalt showed excellent low-temperature properties, elasticity, and flame retardancy [10]. However, polyurethane is expensive, so promoting the use of polyurethane-modified asphalt is difficult. Polyurethane recycled material is processed from polyurethane waste, so it is cheaper than original polyurethane. This type of polyurethane could be used to prepare modified asphalt.

The incorporation of thermoplastic polyurethane recycled material (TPRM) particles into asphalt mixtures may enhance the performance and sustainability of road materials [11,12]. Research has shown that TPRM can improve the mechanical properties of asphalt, such as its durability and resistance to cracking. For instance, Zhang demonstrated that the addition of TPRM particles to asphalt mixtures can increase its load-bearing capacity and resistance to low-temperature cracking [13]. However, it is hard to ensure the compatibility of TPRM with the traditional asphalt components, as the processing temperatures and behaviors differ significantly.

In this study, thermoplastic polyurethane recycled material (TPRM) particles were used to prepare modified asphalt. In order to fully stimulate the TPRM particles, they were mixed with asphalt in advance, and then activated at varying temperatures for different times. After that, modified asphalt was prepared at different shearing temperatures and times [14]. The effects of the shearing/activation temperature and time on high-temperature performance, low-temperature crack resistance, thermal susceptibility, and shear property of the modified asphalt were investigated. Effects of above factors on chemical structures of the modified asphalt were analyzed by using Fourier-transform infrared spectroscopy. The microstructures of the modified asphalt samples prepared at different shearing/activation temperatures and times were investigated using fluorescence microscopy and scanning electron microscopy.

2. Materials and Methods

2.1. Materials

The base asphalt chosen was SK70; its basic indices are shown in Table 1. Twenty-mesh thermoplastic polyurethane recycled material (TPRM) particles were obtained from a shoe factory. The particles are black, with 23.15 wt.% of carbon black.

Table 1. Basic performance of SK70.

Parameter	Result	Standard in China (JTG E20-2011) [15]
Penetration (25 °C, 0.1 mm)	72.5	T0604
Softening point (°C)	48.5	T0606
Ductility (5 °C, cm)	7.40	T0605
Viscosity (135 °C, 18.6 s ^{−1})/Pa·s	0.531	T0625

2.2. Preparation of Modified Asphalt

Modified asphalt is affected by the shearing/activation temperature and time. Thus, the base asphalt was heated until it could flow fully, and 20 wt.% of TPRM was added. Afterwards, these four preparation procedures were followed:

- The mixture of TPRM and asphalt was activated at 170 °C for 60 min, after that it was sheared at 5000 rpm for 60 min. The shearing temperatures were 155 °C, 165 °C, 175 °C, 185 °C, and 195 °C. The modified asphalt with a shearing temperature of 175 °C was named S175, and the other modified asphalt preparations followed the same naming rule.
- The mixture was activated at 170 °C for 60 min. Then, it was sheared at 5000 rpm and 175 °C; the shearing times were 20 min, 40 min, 60 min, 80 min, and 100 min. The modified asphalt with a shearing time of 20 min was named S20, and the other modified asphalt preparations followed the same naming rule.
- The mixture was activated at a certain temperature for 60 min; the activation temperatures were 150 °C, 160 °C, 170 °C, 180 °C, and 190 °C. Then, it was sheared at 5000 rpm and 175 °C for 60 min. The modified asphalt with an activation temperature of 150 °C was named A150, and the other modified asphalt preparations followed the same naming rule.
- The mixture was activated at 170 for 60 min; the activation times were 0 min, 30 min, 60 min, 90 min, and 120 min. Then, it was sheared at 5000 rpm and 175 °C for 60 min. The modified asphalt with an activation time of 0 min was named A0, and the other modified asphalt preparations followed the same naming rule.

2.3. Experiment Methodology

2.3.1. Physical Properties Test

The softening point is usually used to evaluate the high-temperature performance of asphalt according to the Chinese Standards JTG E20-2011 (Test Methods of Asphalt and Asphalt Mixtures for Highway Engineering) [15]. We used $\Phi 55 \times 35$ mm samples with 6 replicates for accuracy. The modified asphalt's hardness was evaluated using a cone penetration test; this method is better than the penetration test for asphalt modified using TPRM particles [16]. Additionally, the shear strength (τ) of asphalt is another evaluation index of asphalt. This was calculated according to Equation (1):

$$\tau = \left[981Q \cos^2(\alpha/2) \right] / \pi h^2 \tan(\alpha/2) \quad (1)$$

where τ represents shear strength, Q denotes the total mass of the loading hammer, α stands for the tip angle of the cone, and h indicates cone penetration. In this study, Q is 150 g, and α is 30° [17]. The cone penetration and shear strength values of SK70 were 55.1 (0.1 mm) and 50.13 kPa, respectively.

2.3.2. Rotational Viscosity

The rotational viscosity of modified asphalt was tested using a Brookfield viscometer at 135 °C, 145 °C, 155 °C, 165 °C, and 175 °C. To ensure the accuracy and reliability of the results, at least three samples were tested in parallel experiments.

2.3.3. Force Ductility Test

In this study, the properties of the modified asphalt prepared at a low temperature were evaluated using the force ductility test (FDT). The sample dimensions were as follows: a total length of 75 mm, 30 mm spacing between the end molds, and minimum cross-sectional dimensions of 10 mm × 10 mm. The test temperature was 5 °C, and the loading rate was 50 mm/min. Three samples were used for testing, and the line closest to the average value was recorded. The area under the FDT curve was calculated, which represents fracture energy. An increase in fracture energy demonstrates the improvement in asphalt at a low temperature.

2.3.4. Fluorescence Microscopy

Fluorescence microscopy (FM, BM2100, Jiangnan, China) was used to investigate the microstructure of the TPRM-modified asphalt. The asphalt samples were dissolved in an appropriate organic solvent to form a uniform, thin film on a glass slide for subsequent analysis. In this study, the FM tests were conducted with a BM2100 microscope; micrographs were taken with a Nikon D7100 camera (D7100, Nikon, Japan), which was equipped with an automatic counter. The modified asphalt was observed at a magnification of 400×.

2.3.5. Fourier-Transform Infrared Spectroscopy Analysis

The difference in chemical structures between the base and modified asphalt were analyzed by Fourier-transform infrared spectroscopy (ATR-FTIR, Bruker TENSOR 27, Germany). During the test, asphalt films were placed on a reflection diamond, and spectra from 400 cm^{−1} to 4000 cm^{−1} were collected at 4 cm^{−1} resolution.

2.3.6. Morphology Analysis

A scanning electron microscope (SEM, Hitachi S4800, Japan) was used to observe the effects of the modifier, the shearing/activation temperatures, and time on the surface morphology of the modified asphalt. The modified asphalt was placed in a refrigerator at −20 °C for 48 h, and then it was taken out and gently broken. The flattest section of the modified asphalt was sputtered with gold under vacuum conditions, and then studied in an SEM test. During this process, the acceleration voltage was 3 kV.

3. Results and Discussion

3.1. Conventional Physical Properties

The effects of shearing/activation temperature and time on the softening points of the modified asphalt are illustrated in Figure 1a,b. In this figure, the softening points increase alongside the shearing/activation temperature and time. These results indicate that the high-temperature performance of the modified asphalt is improved. In addition, the relationship between the softening points and the shearing temperature and time is reflected by the fitting equations shown in Figure 1a. The slope of the curve between the softening point and the shearing temperature is 0.1381, while that between the softening point and the shearing time is 0.1053. Moreover, the relationship between the softening points and the activation temperature and time is reflected by the fitting equations shown in Figure 1b. The slope of the curve between the softening points and the activation temperature is 0.1183, and it is 0.0122 for the softening points and the activation time. The

different curves are ordered as follows: $0.1381 > 0.1183 > 0.1053 > 0.0122$. These results indicate that the shearing temperature improved the modified asphalt's high-temperature performance the most.

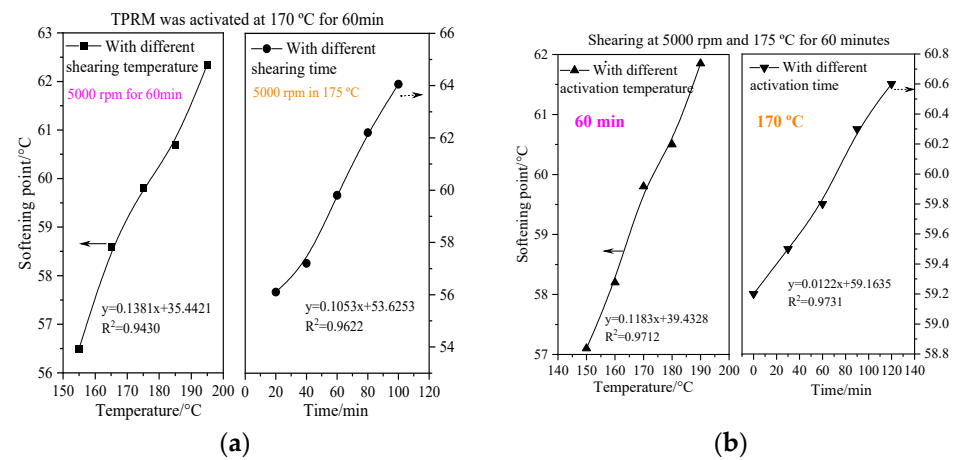


Figure 1. Softening points of modified asphalt (a) at different shearing temperatures and times, and (b) at different activation temperatures and times.

Figure 2a,b show the cone penetration and shear strength results of the modified asphalt at different shearing temperatures and times, respectively, while Figure 2c,d show these results at different activation temperatures and times, respectively. The cone penetration results for the modified asphalt deteriorated with increasing shearing and activation temperatures and during the shearing process. However, the cone penetration results for the modified asphalt improved during activation from 0 min to 60 min, and then it worsened from 60 min to 120 min. The shear strength and cone penetration results exhibited opposite trends. In addition, the cone penetration results for the modified asphalt were consistently worse than those of SK70, while the modified asphalt was consistently stronger than SK70. These results indicate that the modified asphalt was more consistent and stable under pressure and loading than SK70 was.

Additionally, the relationships between the cone penetration results and the shearing/activation temperature and time are represented by the fitting equations shown in Figure 2. The fitting equations of the cone penetration results and the shearing temperature and time and the activation temperature are first-degree polynomial. The fitting equation of the cone penetration results and activation time are quadratic polynomial, with an absolute value of the quadratic coefficient of 0.0026. Figure 2 also shows fitting equations for shear strength and the shearing/activation temperature and time. The fitting equations between shear strength, temperature, and time and the activation temperature are first-degree polynomial. The fitting equation for shear strength and activation time is quadratic polynomial, with an absolute quadratic coefficient of 0.0354. These results indicate that the cone penetration results and shear strength are most sensitive to the activation time, while stability under pressure and loading are also very sensitive to the activation time. In addition, 0.0354 is larger than 0.0026, which indicates that shear strength is more sensitive to the activation time than the cone penetration results are.

At high temperatures, the hydrogen bonds in the hard and soft segments of TPRM broke, leading to less microphase separation and crystallinity. Ultimately, this resulted in the structural weakness of TPRM [18]. Thus, the TPRM particles easily absorbed the light components of asphalt (saturates and aromatics) and swelled, or even dissolved. Under the combined actions of mechanochemical processes and external heating, the molecular chain in TPRM broke, and its structural integrity was destroyed [19]. Thus, the TPRM particles

decreased in size, and the composition of asphalt was changed. As the shearing process continued, more TPRM particles underwent the abovementioned process, and carbon black was released.

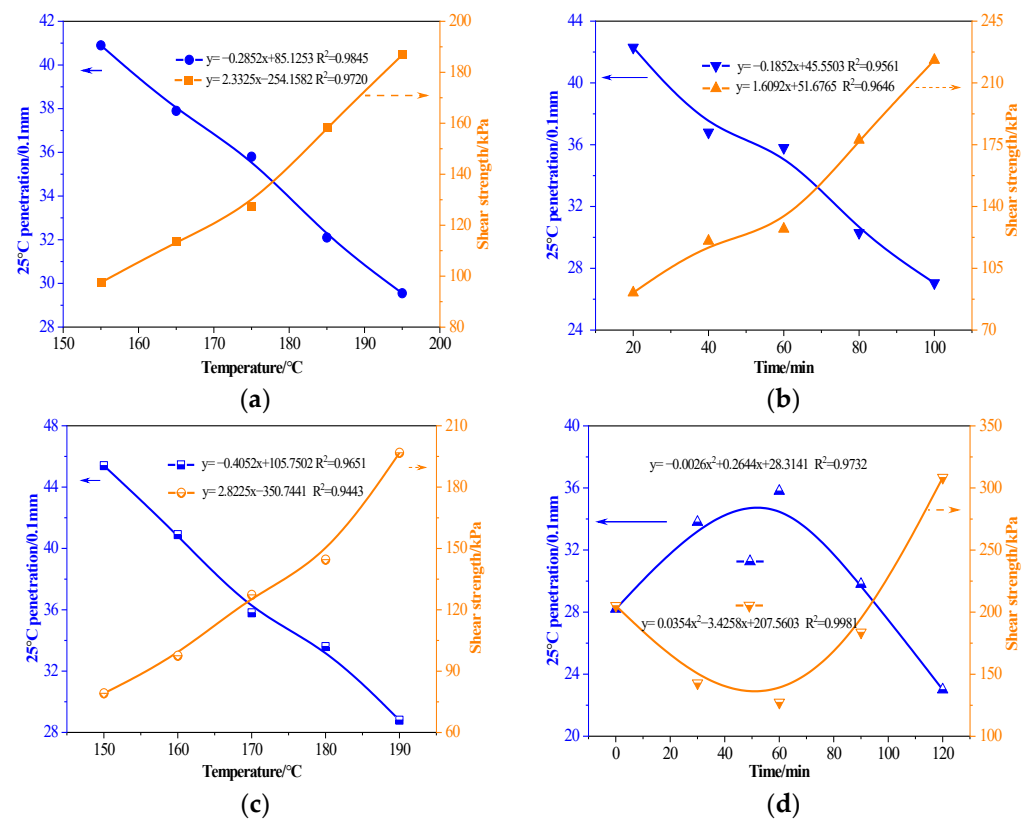


Figure 2. Cone penetration and shear strength results of modified asphalt (a) at different shearing temperatures, (b) at different shearing times, (c) at different activation temperatures, and (d) at different activation times.

As the same time, the asphaltene content in the modified asphalt increased due to aging. Therefore, the surfaces of the TPRM particles absorbing the light components of asphalt formed an asphaltene gel layer with high viscosity. These particles bonded to each other and formed systems of a semi-solid continuous phase with very high viscosity in the modified asphalt. Thus, a “sea–island structure” formed in the modified asphalt matrix [20,21]. The semi-solid continuous phase and the asphalt molecules became attracted to each other, resulting in cohesion and viscosity. Moreover, a part of TPRM formed slender and irregular, fibrous products and dispersed throughout the modified asphalt matrix. The contact area between slender–irregular TPRM and asphalt was large, increasing the resistance of the asphalt molecules and resulting in improved cohesion and viscosity. An increase in the shearing/activation temperature and time accelerated the abovementioned process. Thus, the softening points of the modified asphalt increased with the increase in shearing/activation temperature and time, while the cone penetration results deteriorated with higher shearing and activation temperatures and a longer shearing time. In the modified asphalt matrix, large particles hindered the movement of the cone more than the small particles did. Moreover, the activation of TPRM particles in hot asphalt may have destroyed their structure, shearing them into small particles. Asphalt is prone to aging at high temperatures, and aged asphalt is harder than base asphalt. These phenomena might explain why the cone penetration and shear strength results improved with the increase in activation time.

3.2. Force Ductility

Figure 3 shows FDT curves of SK70 and the modified asphalt. The FDT curves of the modified asphalt are similar to those of SK70. Some researchers conducted a force ductility test in a 5 °C water bath, and they defined the area under the FDT curve as fracture energy. An increase in fracture energy could improve asphalt at low temperatures [22]. The fracture energy of SK70 is 5286/N·mm, and that of the modified asphalt is shown in Figure 4a,b.

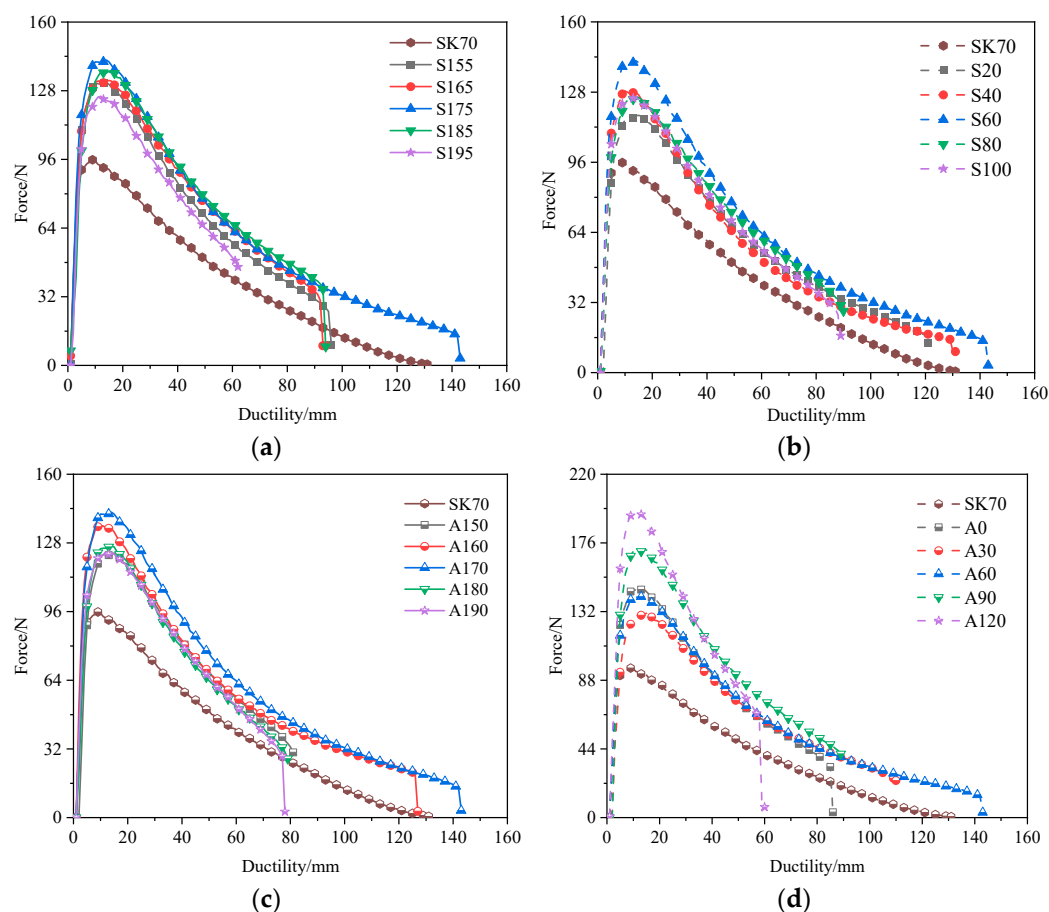


Figure 3. FDT curves of modified asphalt (a) at different shearing temperatures, (b) at different shearing times, (c) at different activation temperatures, and (d) at different activation times.

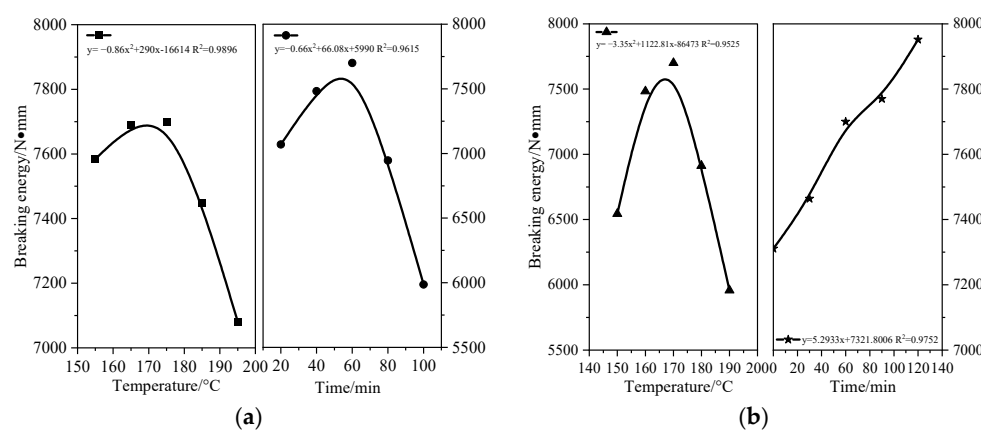


Figure 4. Fracture energy of modified asphalt (a) at different shearing temperatures and times and (b) at different activation temperatures and times.

Figure 4a shows the fracture energy of the modified asphalt at different shearing temperatures and times. The fracture energy of the modified asphalt increased as the shearing temperature increased from 155 °C to 175 °C, and then it decreased from 175 °C to 195 °C. Additionally, the fracture energy of the modified asphalt increased during shearing from 20 min to 60 min, and then decreased from 60 min to 120 min. The fracture energy of the modified asphalt was consistently higher than that of SK70. The relationships between fracture energy and the shearing temperature and time are represented by the fitting equations shown in Figure 4a. The fitting equations between fracture energy and the shearing temperature and time are quadratic polynomials, with absolute quadratic coefficients of 0.8643 and 0.6635, respectively. Figure 4b shows the fracture energy of the modified asphalt at different activation temperatures and times. The fracture energy of the modified asphalt increased as the activation temperature increased from 150 °C to 170 °C, and then it decreased from 170 °C to 190 °C. In addition, the fracture energy of the modified asphalt increased throughout activation. The fracture energy of the modified asphalt was also consistently higher than that of SK70. The relationship between fracture energy and the activation temperature and time is also represented by the fitting equation shown in Figure 4b. The fitting equation between fracture energy and the activation temperature is quadratic polynomial, while that for the activation time is first-degree polynomial. The absolute quadratic coefficient for the fracture energy and activation temperature fitting equation is 3.3502. The order of different quadratic coefficients is as follows: $3.3502 > 0.684 > 0.663$. Thus, the low-temperature crack resistance was most sensitive to changes in activation temperature.

The propagation of cracks is the main reason for the low-temperature fracturing of asphalt materials. According to the crack blocking mechanism, the “sea–island structure” and slender–irregular TPRM could have absorbed the stress and strain energy present in the modified asphalt under tension, thereby increasing its fracture energy [23,24]. Additionally, the reinforcing effect of carbon black might have also contributed to the increase in fracture energy [25]. As the shearing temperature and time and the activation temperature increase, the “sea–island structure” and slender–irregular TPRM became more prominent. However, asphalt is prone to aging with an increase in the shearing temperature and time and the activation temperature, and aged asphalt is brittle and easily cracks at low temperatures. These factors are the reason that the fracture energy showed opposite trends with the increasing shearing temperature and time and activation temperature. As the activation time increased, the “sea–island structure” of the modified asphalt also gradually emerged, and the amount of slender–irregular TPRM also increased. However, the asphalt did not age enough to cause a significant decrease in fracture energy, even as the activation time increased. Therefore, the fracture energy of the modified asphalt increased during activation. Furthermore, the activation temperature had a significant effect on the swelling of TPRM particles, but it did not cause the serious aging of asphalt, which might be the reason why low-temperature crack resistance is the most sensitive to the change in activation temperature.

3.3. Thermal Susceptibility

Figure 5a,b show the viscosity of the modified asphalt at different shearing temperatures and times. The modified asphalt became less viscous as the test temperature increased. However, it became more viscous as the shearing temperature and time increased. Figure 5c,d show the viscosity of the modified asphalt at the different activation temperatures and times. Similarly, the modified asphalt also became less viscous as the test temperature increased. Moreover, there was no obvious difference in the viscosity of the modified asphalt at the different activation temperatures. However, modified asphalt

became less viscous during activation from 0 min to 60 min, and then it became more viscous from 60 min to 120 min.

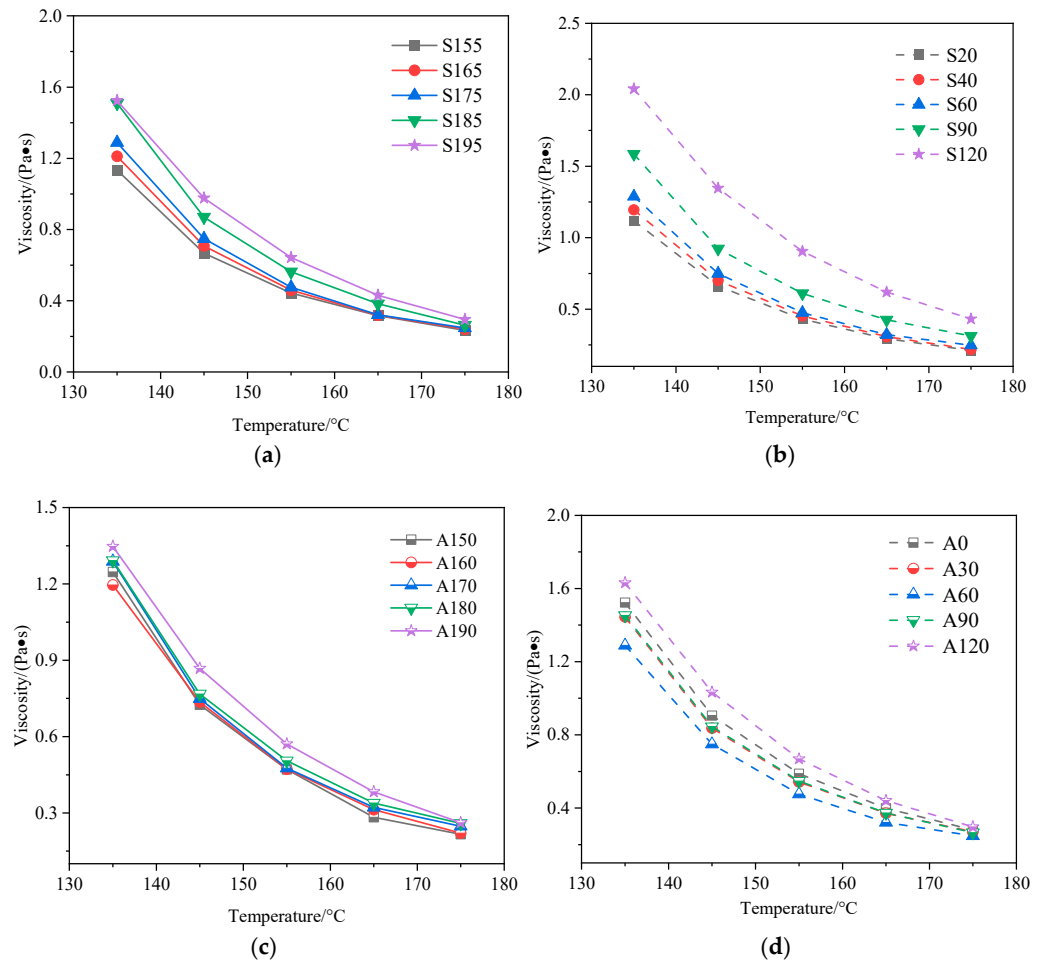


Figure 5. Viscosity changes in modified asphalt (a) at different shearing temperatures, (b) at different shearing times, (c) at different activation temperatures, and (d) at different activation times.

Equation (2) is an Arrhenius equation, which is usually used to describe the viscosity–temperature relationship of asphalt:

$$\eta(T) = A \bullet e^{-E\eta/RT} \quad (2)$$

where η is defined as viscosity, Pa·s; A represents the regression coefficient; $E\eta$ denotes viscous activation energy, J/mol; R stands for the universal gas constant, $8.314 \text{ J} \cdot \text{mol}^{-1} \cdot \text{K}^{-1}$; and T indicates absolute temperature, K.

$E\eta$ was used to characterize the thermal susceptibility of the modified asphalt according to Equation (3):

$$\text{Log } \eta(T) = \text{Log } A + E\eta/2.303RT \quad (3)$$

Equation (3) indicates that $\text{Log } \eta$ has a linear relationship with $1/T$. The data in Figure 5 were plotted in $\text{Log } \eta(T)-1/T$ form; the results are presented in Figure 6. The slope of the straight line is $E\eta/2.303R$. Then, the $E\eta$ of modified asphalt was calculated. The fitting results and $E\eta$ are shown in Table 2.

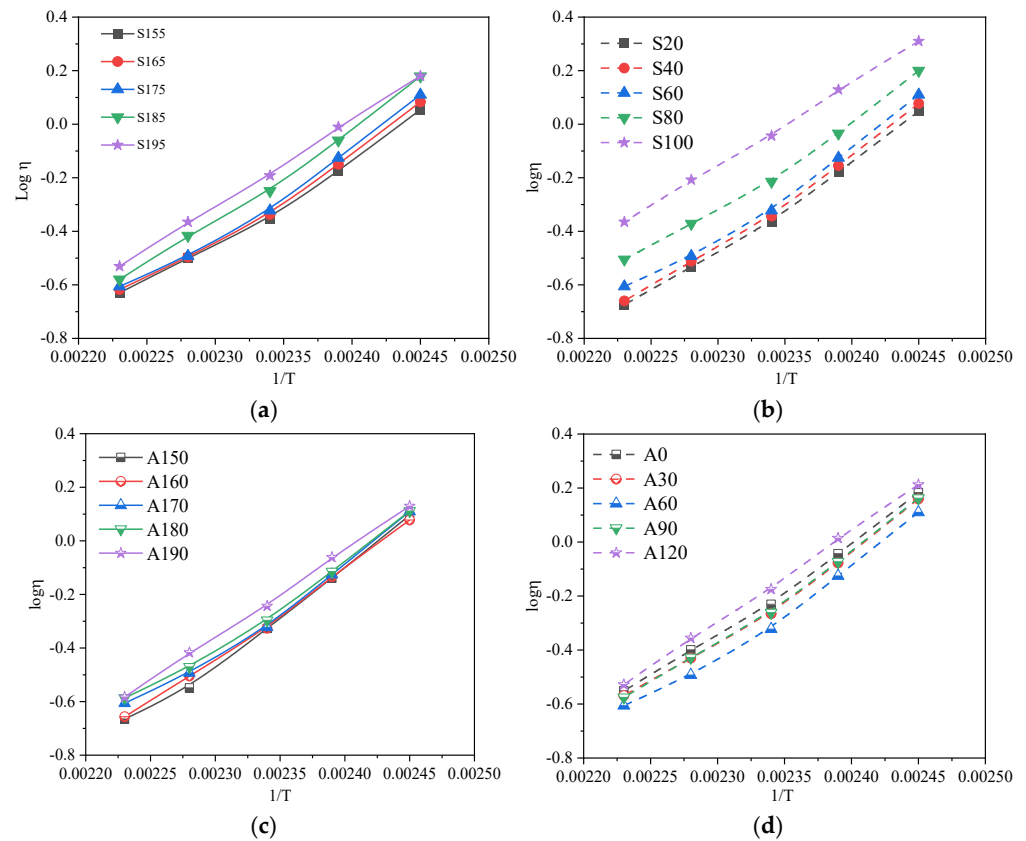


Figure 6. $\text{Log} \eta \sim 1/T$ relationship curves of modified asphalt (a) at different shearing temperatures, (b) at different shearing times, (c) at different activation temperatures, and (d) at different activation times.

Table 2. $\text{Log} \eta \sim 1/T$ linear fitting results.

No.	Viscosity–Temperature Relationship	$E\eta/\text{kJ} \cdot \text{mol}^{-1}$	Correlation Coefficient R^2
S155	$\text{Log} \eta = 3012.7080/T - 7.3765$	57.6847	0.9834
S165	$\text{Log} \eta = 3151.1554/T - 7.4934$	60.3356	0.9839
S175	$\text{Log} \eta = 3233.2292/T - 7.9966$	61.9071	0.9991
S185	$\text{Log} \eta = 3295.9540/T - 7.8818$	63.1081	0.9948
S195	$\text{Log} \eta = 3250.2511/T - 7.7832$	62.2330	0.9898
S20	$\text{Log} \eta = 3191.8295/T - 7.8111$	61.1144	0.9927
S40	$\text{Log} \eta = 3269.3270/T - 7.9338$	62.5982	0.9922
S60	$\text{Log} \eta = 3285.4456/T - 7.9966$	62.9071	0.9791
S80	$\text{Log} \eta = 3253.6819/T - 7.5300$	62.2987	0.9921
S100	$\text{Log} \eta = 3134.1856/T - 7.2518$	60.0108	0.9932
A150	$\text{Log} \eta = 3338.9564/T - 8.1265$	63.9314	0.9934
A160	$\text{Log} \eta = 3308.1347/T - 8.0493$	63.3413	0.9931
A170	$\text{Log} \eta = 3288.2562/T - 7.9966$	62.9071	0.9891
A180	$\text{Log} \eta = 3267.7675/T - 7.9248$	62.5684	0.9951
A190	$\text{Log} \eta = 3258.3283/T - 7.8536$	62.3876	0.9958
A0	$\text{Log} \eta = 3304.4583/T - 7.9465$	63.2709	0.9951
A30	$\text{Log} \eta = 3265.6680/T - 7.8502$	62.5282	0.9832
A60	$\text{Log} \eta = 3269.7940/T - 7.9966$	62.6071	0.9991
A90	$\text{Log} \eta = 3302.9656/T - 7.9675$	63.2423	0.9792
A120	$\text{Log} \eta = 3385.87562/T - 8.0831$	64.8298	0.9993

As presented in Table 2, the correlation coefficient of the linear fitting curve is above 0.9, showing a good linear relationship between $\log \eta$ and $1/T$. The slope of the line reflects the sensitivity of viscosity changes to temperature; its value is usually used to reflect the difference in $E\eta$ [26]. In addition, fitting curves between $E\eta$ and the shearing/activation temperature and time are shown in Figure 7.

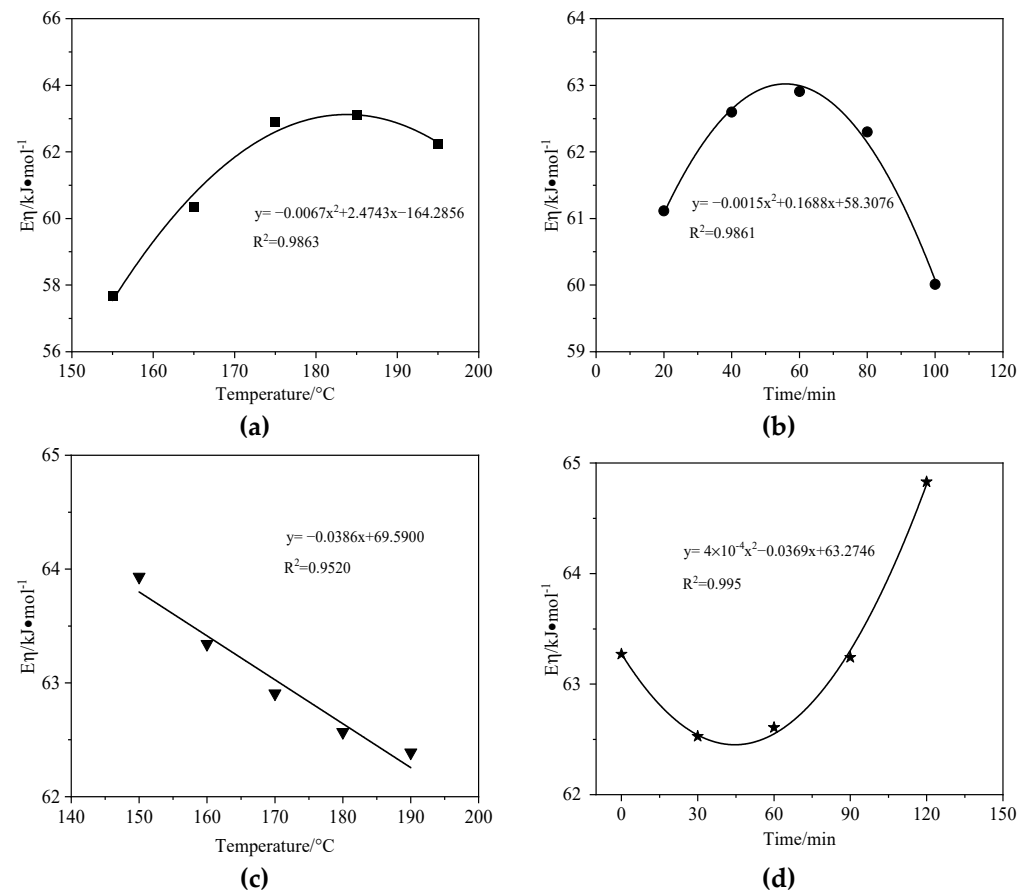


Figure 7. Fitting curves (a) between $E\eta$ and shearing temperature, (b) between $E\eta$ and shearing time, (c) between $E\eta$ and activation temperature, and (d) between $E\eta$ and activation time.

$E\eta$ increased as the shearing temperature increased from 155 °C to 175 °C, and then it decreased from 175 °C to 195 °C. Moreover, $E\eta$ increased with the shearing time increase from 20 min to 60 min, and then it decreased from 60 min to 120 min. $E\eta$ decreased with an increasing activation temperature. $E\eta$ decreased first, and thereupon increased with an increasing activation time. It was worth mentioning that $E\eta$ and thermal susceptibility show opposite trends. In addition, the fitting equations between $E\eta$ and the shearing temperature and time and activation time are quadratic polynomial, while the fitting equations between $E\eta$ and the activation temperature are first-degree polynomial. The absolute quadratic coefficients of the fitting curves between $E\eta$ and the shearing temperature and time and activation time are 0.0067, 0.0015, and 0.0004, respectively. Thus, $E\eta$ is the most sensitive to shearing temperature, which means that thermal susceptibility is the most sensitive to the shearing temperature.

As the shearing temperature and time increased, the asphalt showed obviously aged, the ‘sea–island structure’ became more prominent, and the amount of slender–irregular TPRM increased as the regular TPRM particles dissolved. These changes made the intermolecular force and the interface viscosity stronger. Modified asphalt must overcome a high energy barrier. However, maintaining an overly high shearing temperature over a long time caused the excessive volatilization of the light components of asphalt. Addition-

ally, the TPRM particles absorbed fewer light components of asphalt; thus, the interface effect between the asphalt molecules and the regular and slender-irregular TPRM particles weakened. These factors caused increased thermal susceptibility. Moreover, the TPRM particles swelled more with an increasing activation temperature, and the TPRM particles in the modified asphalt became smaller with an increasing activation temperature. The large TPRM particles in asphalt could not move as easily as the small TPRM particles could. The modified asphalt with a low activation temperature needed to overcome high energy barriers when moving. Thus, thermal susceptibility increased with an increasing activation temperature. The TPRM particles also swelled more during activation, while their size decreased. These factors may explain why the thermal susceptibility of the modified asphalt with an activation time of 30 min was higher than that with no activation. Additionally, the content of heavy components in modified asphalt increased with the increasing activation time, the 'sea-island structure' developed, and the amount of slender-irregular TPRM also increased. Under the combined effect of the abovementioned factors, thermal susceptibility decreased as the activation time increased from 30 min to 120 min. Furthermore, the effects of the change in shearing temperature on the structure of the TPRM particles and the degree of asphalt aging likely contributed to thermal susceptibility, which was most sensitive to the shearing temperature.

3.4. FM

The FM results of the modified asphalt are shown in Figure 8, where the light parts of the picture represents TPRM. There are lots of TPRM particles dispersed in S155, varying a lot in size. As the shearing temperature increased to 165 °C, TPRM became dispersed in the modified asphalt as a flocculent continuous phase, and some TPRM particles were also observed. Otherwise, the dispersion of TPRM particles in S155 and S165 was poor. In S175, lots of smaller TPRM particles were relatively evenly dispersed in the modified asphalt, and flocculent TPRM was not found. The TPRM particles absorbed the light components of asphalt at a high temperature, and these particles showed obvious swelling, and even dissolution. As the shearing temperature increased, the swelling and dissolution degree of the TPRM particles increased.

Under the activation of shearing force, the swollen TPRM particles became smaller, and soluble TPRM evenly dispersed in the modified asphalt. These changes might have resulted in the morphology change in the modified asphalt, with the shearing temperature increasing from 155 °C to 175 °C. However, the modified asphalt showed no significant difference in morphology with the shearing temperature increasing from 175 °C to 195 °C. Moreover, the TPRM particles in S20 were larger than those in S155, and the TPRM particles are less bright from the center to the edge. These differences could be due to the outer layers of TPRM particles absorbing more of the light components of asphalt compared to the center of the TPRM particles. Moreover, flocculent TPRM was also found in S40. The TPRM particles in S20 and S40 are unevenly dispersed. As the shearing time increased from 60 min to 100 min, lots of smaller TPRM particles were relatively evenly dispersed in the modified asphalt, while flocculent TPRM was not found. These results might explain why the degree of mutual penetration of the light components of asphalt and TPRM increased as the shearing time increased. These TPRM particles were partially dissolved under the action of shearing force and evenly dispersed in the modified asphalt.

In A150, the TPRM particles were larger than those in S20, and there was no significant difference in brightness between the centers and edges of the TPRM particles. This was because the TPRM particles absorbed fewer light components of asphalt at a low temperature, and the difference in the degree of swelling between the centers and the edges of TPRM particles was low. In A160, the TPRM particles were obviously smaller than

those in A150, and flocculent TPRM was distributed around the TPRM particles. This indicates that the swelling or dissolution degree of the particles in A160 was greater than those in A150, and they were more easily sheared into smaller particles. Furthermore, the TPRM particles were unevenly distributed in A150 and A160. When the activation temperature was above 160 °C, the TPRM particles in the modified asphalt became smaller than those in A160, and the TPRM particles in the modified asphalt were significantly more uniformly dispersed. However, the morphology of the modified asphalt did not change as the activation temperature increased from 170 °C to 190 °C. Moreover, the TPRM particles in A0 were larger than those in A150, which could explain why the TPRM particles did not activate. The TPRM particles in A30 were smaller than those in A0, and they were less bright than those in A0. This could be because the TPRM particles in A30 were more swollen than those in A0. In addition, the TPRM particles were poorly dispersed in A0 and A30. The TPRM particles in S175 were smaller than those in A30, and they were significantly more dispersed. Subsequently, the further increase in activation time had little effect on the TPRM particles' size or dispersibility.

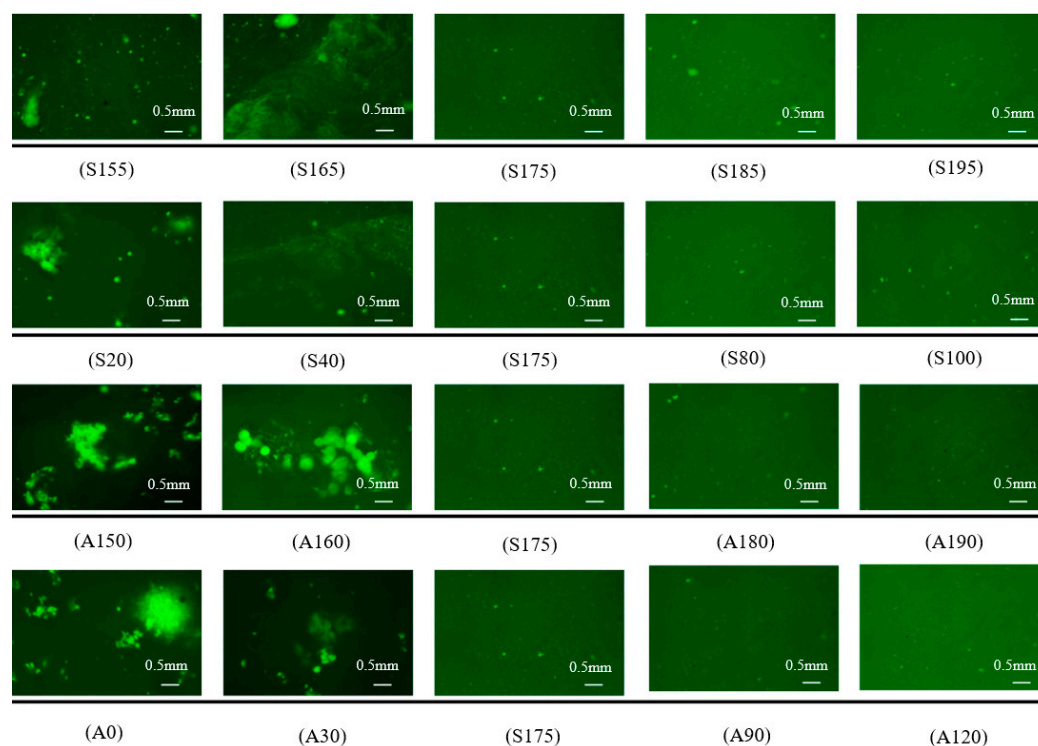


Figure 8. FM results of different modified asphalt samples.

3.5. FTIR

Figure 9a shows the FTIR spectra of TPRM and SK70, indicating that these materials are quite different. The peak at 3545 cm^{-1} observed in TPRM could be assigned to the N-H group, and the strong peaks of TPRM and SK70 between 2850 and 2930 cm^{-1} relate to the $-\text{CH}_2$ group. Additionally, the strong transmission peaks of TPRM at approximately 1700 and 1728 cm^{-1} are related to C=O in urethane. The peak at 1700 cm^{-1} is a characteristic peak of C=O forming a hydrogen bond, while the peak at 1728 cm^{-1} is a characteristic peak of C=O without hydrogen bond formation [27,28]. Finally, the peaks at 1453 and 1375 cm^{-1} relate to C-H bonds.

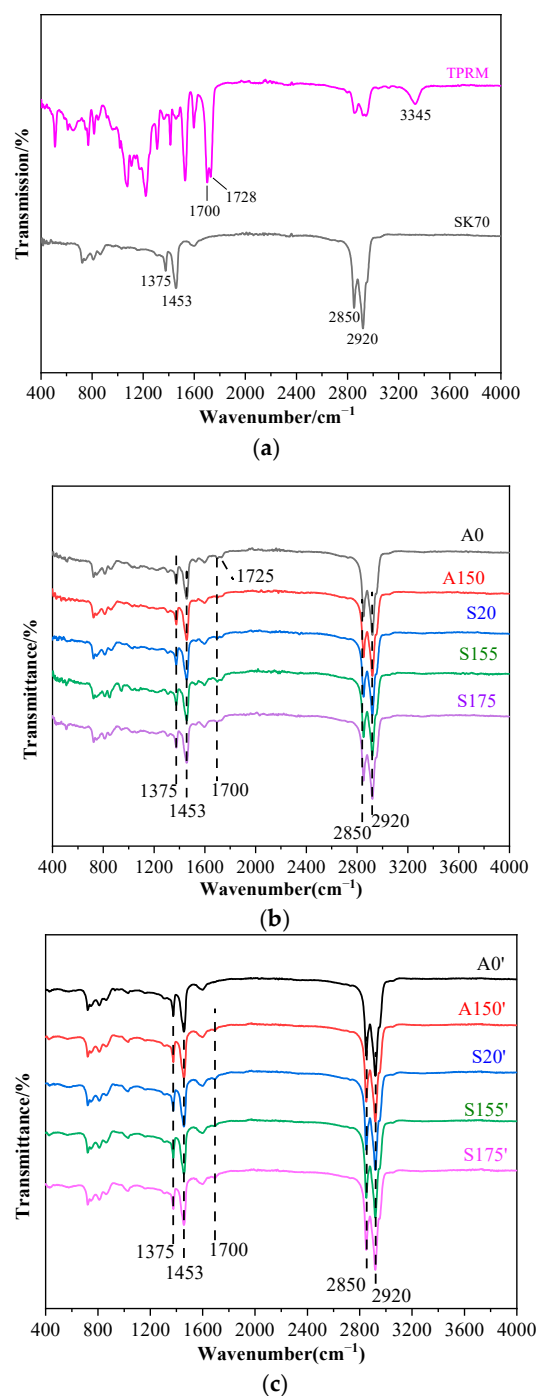


Figure 9. FTIR results of raw materials and modified asphalt: (a) TPRM and SK70; (b) A0, A150, S20, S155, and S175; and (c) A0', A150', S20', S155', and S175'.

Based on the above analysis, S175 showed the most excellent physical properties. Thus, the chemical structures of A0, A150, S20, S155, and S175 were analyzed by FTIR to investigate the effects of the shearing/activation temperature and time on the chemical structures of the modified asphalt. The FTIR spectra of A0, A150, S20, S155, and S175 are presented in Figure 9b. The FTIR spectra of the modified asphalt samples were the same. These results indicate that the modified asphalt samples have similar chemical structures. Compared to the FTIR spectra of SK70, two new transmission peaks in the range of 1700–1730 cm⁻¹ were observed in the FTIR spectra of the modified asphalt. They relate to the C=O bond in TPRM. Additionally, to simulate the effects of shearing and activation processes on the chemical structure of the base asphalt, SK70 underwent the same shearing

and activation processes as the modified asphalt. A0' represents the asphalt that had no modifier and underwent the same activation and shearing process to A0, and the same naming rule was also applied to A150', S20', S155', and S175'. Figure 9c shows the FTIR spectra of A0', A150', S20', S155', and S175'. This asphalt had a similar chemical structure to the base asphalt shown in Figure 9a, while the intensity of peak at 1700 cm^{-1} increased with the increasing shearing/activation temperature and time. This could be related to the aging phenomenon of asphalt.

In order to gain a comprehensive understanding of the chemical structure of the modified asphalt, the following indices were calculated using Equation (4).

$$I = A_{1700} / A_{2850-2930} \quad (4)$$

where A_{1700} represents the peak area of the C=O at 1700 cm^{-1} . $A_{2850-2930}$ denotes the peak area between 2850 and 2930 cm^{-1} [29]. The I of the asphalt without a modifier is donated as I_{UN} , and the I of the modified asphalt is donated as I_{MD} . R stands for the ratio between I_{UN} and I_{MD} , and this was acquired using Equation (5).

$$R = I_{UN} / I_{MD} \quad (5)$$

R_0 represents the ratio between the I_{UN} of A0' and the I_{MD} of A0. R_{150} , R_{20} , R_{155} , and R_{175} follow the same naming rule. I_{UN} , I_{MD} , and R are shown in Figure 10.

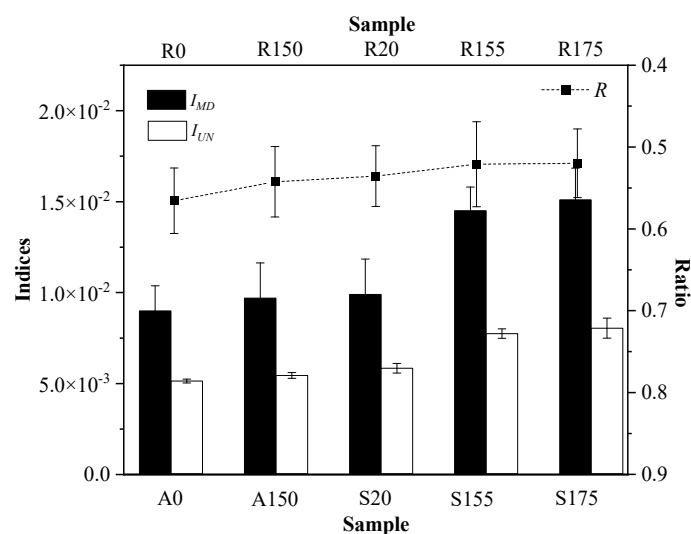


Figure 10. I and R values.

The modified asphalt with a higher shearing/activation temperature had larger I_{UN} and I_{MD} values, while R decreased as the shearing/activation temperature and time increased. During the cooling process of the hot, modified asphalt, the polyurethane molecules had sufficient time to relax and re-orientate, causing microphase separation. This process is conducive to the formation of hydrogen bonds in TPRM [30]. The trend of R is also connected with the hydrogen bonds formed between C=O in TPRM and the polar functional group of asphaltene [25,31–34].

3.6. SEM

SEM images of SK70, A0, A150, S20, S155, and S175 are shown in Figure 11. The section of SK70 has a relatively flat, homogeneous structure, with a smooth surface. In contrast, the modified asphalt samples displayed heterogeneous structures, with a distinct hilly and gully microstructure. Additionally, the TPRM particles were distributed within the

modified asphalt. This indicates the formation of a ‘sea–island structure’ in the modified asphalt matrix. Moreover, the particle sizes in the different modified asphalt samples varied, following this order: A0 > A150 > S20 > S155 > S175.

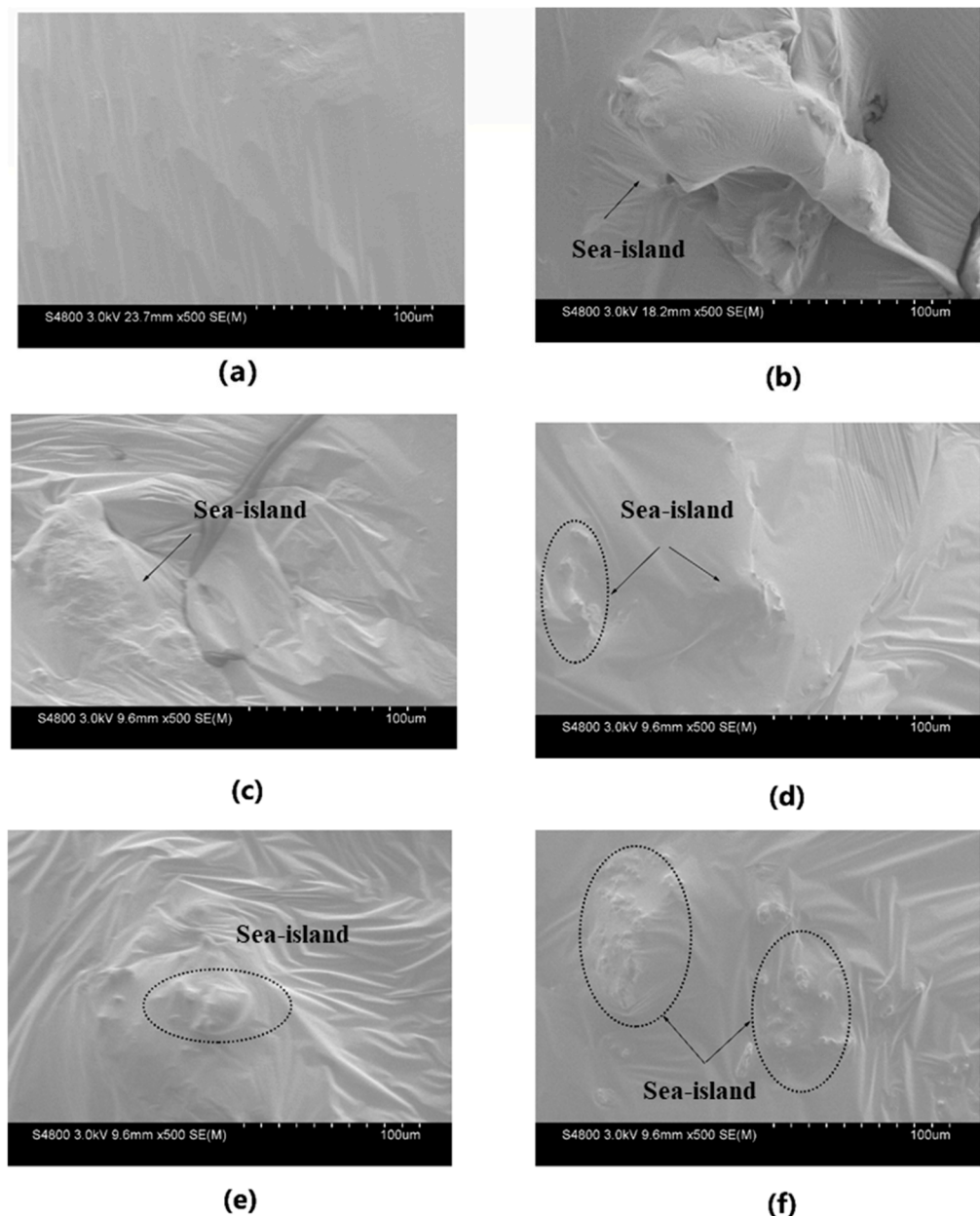


Figure 11. SEM results of SK70 and modified asphalt: (a) SK70, (b) A0, (c) A150, (d) S20, (e) S155, and (f) S175.

Figure 12 also shows the microstructure of the modified asphalt; lots of slender–irregular TPRM particles were distributed within the modified asphalt matrix, disrupting the continuity of the hilly and gully structure. During activation, the TPRM particles absorbed the light components of asphalt, swelled, and then sheared into smaller particles. As a result, the TPRM particles in A0 are larger than those in S175. The longer shearing time and higher temperature in S175 compared to those for S20 resulted in smaller TPRM particles in S175. Despite S155 having a lower shearing temperature than S20, its longer shearing time produced smaller TPRM particles than those in S20. These findings suggest that the shearing time had a greater impact on TPRM particle size than temperature did. Additionally, while A0 and A150 underwent the same shearing conditions, the TPRM

particles in A0 were larger than those in A150, indicating that the activation process reduced the particle size.

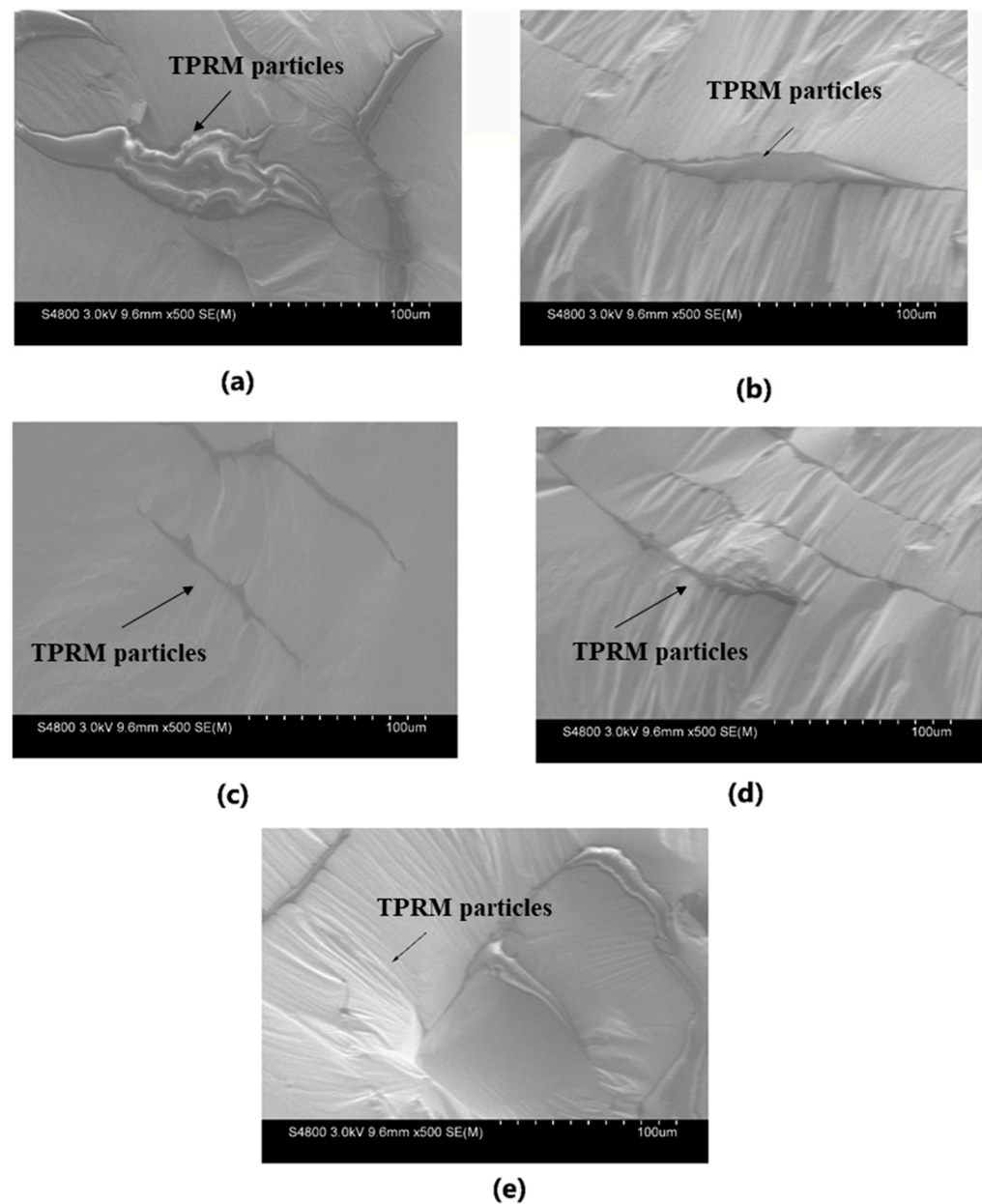


Figure 12. SEM results of modified asphalt: (a) A0, (b) A150, (c) S20, (d) S155, and (e) S175.

Moreover, A0 (without activation) and S20 (with activation) were exposed to the same shearing temperature, but the shearing time for S20 was shorter than that for A0. Despite this, the TPRM particles in A0 were larger than those in S20, indicating that the activation process had a greater impact on particle size than the shearing time did. However, under the action of shearing force, slender-irregular TPRM was obtained and dispersed in the modified asphalt matrix. These TPRM particles blocked the continuity of the hilly and gulley structure in the modified asphalt matrix, which made it more stable [24,35]. Additionally, the substantial mechanical force between the sawtooth TPRM particles and the asphalt matrix hindered the movement of asphalt molecules. Thus, the physical properties of asphalt were improved. The presence of a hilly and gulley structure in the modified asphalt caused plastic deformation in the matrix, which increased the energy required for

crack growth at low temperatures. This might be the reason for the improvement in the low-temperature crack resistance of asphalt.

4. Conclusions

Asphalt modified with thermoplastic polyurethane recycled material (TPRM) particles was successfully prepared. The effects of shearing/activation temperature and duration on the high-temperature performance, low-temperature crack resistance, thermal susceptibility, and shear properties of the modified asphalt were investigated. The chemical structure and microstructure of the modified asphalt at different shearing/activation temperatures and times were investigated to determine the optimal processes and mechanisms. Based on the above results and discussion, the following conclusions can be drawn:

- (1) The swelling and dissolution of TPRM particles altered the composition of asphalt; small and slender-irregular TPRM particles caused increased cohesion and low-temperature fracture energy level. These changes led to an improved high-temperature performance and the better low-temperature crack resistance of the modified asphalt. The shearing temperature was identified as the primary factor in improving high-temperature performance, while the activation temperature impacted low-temperature crack resistance.
- (2) The thermal susceptibility of the modified asphalt was influenced by the extent of the swelling and dissolution of TPRM particles. This was also related to the composition of asphalt and the interface effect between the asphalt molecules and the slender-irregular TPRM particles. Additionally, the thermal susceptibility of the modified asphalt was very sensitive to the shearing temperature.
- (3) At high temperatures, the TPRM particles absorbed the light components of asphalt, resulting in significant swelling and dissolution. The TPRM particles became smaller with an increasing shearing/activation temperature and time. As the shearing/activation temperature and time increased, these particles in the modified asphalt uniformly dispersed. The activation temperature and time had a more pronounced effect on the swelling and dissolution of TPRM particles.
- (4) The increase in shearing/activation temperature and time led to an increase in the hydrogen bond content of the modified asphalt. Small, slender-irregular TPRM particles that formed a hilly or gulley structure were observed in the modified asphalt matrix. These microstructures enhanced the high-temperature performance and low-temperature crack resistance of the modified asphalt.

Author Contributions: Conceptualization, P.Y.; methodology, P.Y.; validation, P.C., H.H. and P.X.; formal analysis, P.Y.; investigation, P.Y.; resources, P.C.; data curation, P.Y.; writing—original draft preparation, P.Y.; writing—review and editing, P.Y., P.C., H.H. and P.X. All authors have read and agreed to the published version of the manuscript.

Funding: This research was funded by the National Natural Science Foundation of China (51978070) and the Shaanxi Natural Science Basic Research Project (2020JM-265).

Data Availability Statement: All of the data, models, and code generated or used during the study appear in the submitted article.

Conflicts of Interest: The authors declare no conflicts of interest. Author Peng Yang was employed by Guangdong Key Laboratory of Materials and Equipment in Harsh Marine Environment. Author Pengfei Xiong was employed by Guangdong Communication Planning & Design Institute Group Co., Ltd. The remaining authors declare that the research was conducted in the absence of any commercial or financial relationships that could be construed as a potential conflict of interest.

Abbreviations

The following abbreviations are used in this manuscript:

TPRM Thermoplastic polyurethane recycled material

References

- Polacco, G.; Filippi, S.; Merusi, F.; Stastna, G. A review of the fundamentals of polymer-modified asphalt: Asphalt/polymer interactions and principles of compatibility. *Adv. Colloid Interfac.* **2015**, *224*, 72–112. [CrossRef] [PubMed]
- Lesueur, D. The colloidal structure of bitumen: Consequences on the rheology and on the mechanisms of bitumen modification. *Adv. Colloid Interfac.* **2009**, *145*, 42–82. [CrossRef] [PubMed]
- Ryms, M.; Denda, H.; Jaskuła, P. Thermal stabilization and permanent deformation resistance of LWA/PCM-modified asphalt road surfaces. *Constr. Build. Mater.* **2017**, *142*, 328–341. [CrossRef]
- Qian, C.; Fan, W.; Yang, G.; Han, L.; Xing, B.; Lv, X. Influence of crumb rubber particle size and SBS structure on properties of CR/SBS composite modified asphalt. *Constr. Build. Mater.* **2020**, *235*, 117517. [CrossRef]
- Xu, L.; Li, X.; Zong, Q.; Xiao, F. Chemical, morphological and rheological investigations of SBR/SBS modified asphalt emulsions with waterborne acrylate and polyurethane. *Constr. Build. Mater.* **2021**, *272*, 121972. [CrossRef]
- Padhan, R.K.; Sreeram, A. Enhancement of storage stability and rheological properties of polyethylene (PE) modified asphalt using cross linking and reactive polymer based additives. *Constr. Build. Mater.* **2018**, *188*, 772–780. [CrossRef]
- Liang, M.; Ren, S.; Fan, W.; Xin, X.; Shi, J.; Luo, H. Rheological property and stability of polymer modified asphalt: Effect of various vinyl-acetate structures in EVA copolymers. *Constr. Build. Mater.* **2017**, *137*, 367–380. [CrossRef]
- Sun, M.; Zheng, M.; Qu, G.; Yuan, K.; Bi, Y.; Wang, J. Performance of polyurethane modified asphalt and its mixtures. *Constr. Build. Mater.* **2018**, *191*, 386–397. [CrossRef]
- Jin, X.; Guo, N.; You, Z.; Wang, L.; Wen, Y.; Tan, Y. Rheological properties and micro-characteristics of polyurethane composite modified asphalt. *Constr. Build. Mater.* **2020**, *234*, 117395. [CrossRef]
- Xia, L.; Cao, D.; Zhang, H.; Guo, Y. Study on the classical and rheological properties of castor oil-polyurethane pre polymer (C-PU) modified asphalt. *Constr. Build. Mater.* **2016**, *112*, 949–955. [CrossRef]
- Ashish, P.K.; Sreeram, A.; Xu, X.; Chandrasekar, P.; Jagadeesh, A.; Adwani, D.; Padhan, R.K. Closing the Loop: Harnessing waste plastics for sustainable asphalt mixtures—A comprehensive review. *Constr. Build. Mater.* **2023**, *400*, 132858. [CrossRef]
- Cong, P.; Liu, C.; Han, Z.; Zhao, Y. A comprehensive review on polyurethane modified asphalt: Mechanism, characterization and prospect. *J. Road Eng.* **2023**, *3*, 315–335. [CrossRef]
- Zhang, T.; Hu, K.; Chen, Y.; Zhang, W.; Gillani, S.T.A.; Qiao, Z. Feasibility and environmental assessment of introducing waste polyurethane from wind turbine blades as a modifier for asphalt. *Constr. Build. Mater.* **2024**, *446*, 138052. [CrossRef]
- Jia, M.; Zhang, Z.; Liu, H.; Peng, B.; Zhang, H.; Lv, W.; Zhang, Q.; Mao, Z. The synergistic effect of organic montmorillonite and thermoplastic polyurethane on properties of asphalt binder. *Constr. Build. Mater.* **2019**, *229*, 116867. [CrossRef]
- JTG E20-2011; Test Methods of Asphalt and Asphalt Mixtures for Highway Engineering. Ministry of Transport of the People's Republic of China: Beijing, China, 2011.
- Zheng, W.; Wang, H.; Chen, Y.; Ji, J.; You, Z.; Zhang, Y. A review on compatibility between crumb rubber and asphalt binder. *Constr. Build. Mater.* **2021**, *297*, 123820. [CrossRef]
- Lei, Y.; Wang, H.; Chen, X.; Yang, X.; You, Z.; Dong, S.; Gao, J. Shear property, high-temperature rheological performance and low-temperature flexibility of asphalt mastics modified with bio-oil. *Constr. Build. Mater.* **2018**, *174*, 30–37. [CrossRef]
- Wang, T.; Yang, R.; Li, A.; Chen, L.; Zhou, B. Experimental research on applying shear strength of cone penetration to performance evaluation of rubber asphalt. *J. Hefei Univ. Technol.* **2016**, *39*, 380–384.
- Yilgör, E.; Yurtsever, E.; Yilgör, I. Hydrogen bonding and polyurethane morphology. II. Spectroscopic, thermal and crystallization behavior of polyether blends with 1,3-dimethylurea and a model urethane compound. *Polymer* **2002**, *43*, 6561–6568. [CrossRef]
- Wu, Z.; Lui, G.; Lui, Z.; Yang, X.; Pan, S. Numerical simulation and experimental study on recycle of waste thermosetting polyurethane. *China Plast.* **2012**, *26*, 93–98. (In Chinese) [CrossRef]
- Chen, Y.; Wang, W.; Yuan, D.; Xu, C.; Cao, L.; Liang, X. Bio-Based PLA/NR-PMMA/NR Ternary TPVs with Balanced Stiffness and Toughness: “Soft-Hard” Core-Shell Continuous Rubber Phase, In-Situ Compatibilization and Properties. *ACS Sustain. Chem. Eng.* **2018**, *6*, 6488–6496. [CrossRef]
- Antunes, C.; Machado, A.; van Duin, M. Morphology development and phase inversion during dynamic vulcanisation of EPDM/PP blends. *Eur. Polym. J.* **2011**, *47*, 1447–1459. [CrossRef]
- Du, Z.Y.; Yuan, J.; Xiao, F.P. Improvement of low temperature performance evaluation method of LDPE modified asphalt. *J. Build. Mater.* **2020**, *9*, 1–16. Available online: <https://kns.cnki.net/kcms/detail/31.1764.TU.20200927.0852.002.html> (accessed on 27 September 2020). (In Chinese)

24. Cam, J.; Toussaint, E. The Mechanism of Fatigue Crack Growth in Rubbers under Severe Loading: The Effect of Stress-Induced Crystallization. *Macromolecules* **2010**, *43*, 4708–4714. [[CrossRef](#)]
25. Hua, Y.Q.; Jin, R.G. *Polymer Physics*; Chemical Industry Press: Beijing, China, 2013; pp. 235–237.
26. Dong, W.Z. *Study on Properties of Carbon Black/Thermoplastic Polyurethanes Composite Modified Asphalt*; Changsha University of Science & Technology: Changsha, China, 2020. (In Chinese)
27. Jiang, X.; Li, P.; Ding, Z.; Yang, L.; Zhao, J. Investigations on viscosity and flow behavior of polyphosphoric acid (PPA) modified asphalt at high temperatures. *Constr. Build. Mater.* **2019**, *228*, 116610. [[CrossRef](#)]
28. Trong-Ming, D.; Chiu, W.; Hsieh, K. The Thermal Aging of Filled Polyurethane. *J. Appl. Polym. Sci.* **1991**, *43*, 2193–2199. [[CrossRef](#)]
29. Yang, H.; Wang, X.P.; Zheng, J. The aging mechanism of thermoplastic polyurethane elastomer. *J. Xiamen Univ. Nat. Sci.* **2017**, *56*, 370–377. (In Chinese)
30. Cong, P.; Guo, X.; Mei, L. Investigation on rejuvenation methods of aged SBS modified asphalt binder. *Fuel* **2020**, *279*, 118556. [[CrossRef](#)]
31. Li, Z.F.; Zhang, T.L.; Xu, C.M. Study on effect of thermal process on the morphology and mechanical properties of RIMPUU by In-situ FTIR. *Spectrosc. Spectr. Anal.* **2004**, *24*, 1066–1068. (In Chinese)
32. Cong, L.; Yang, F.; Guo, G.; Ren, M.; Shi, J.; Tan, L. The use of polyurethane for asphalt pavement engineering applications: A state-of-the-art review. *Constr. Build. Mater.* **2019**, *225*, 1012–1025. [[CrossRef](#)]
33. Martín-Alfonso, M.; Partal, P.; Navarro, F.; García-Morales, M.; Bordado, J.; Diogo, A. Effect of processing temperature on the bitumen/MDI-PEG reactivity. *Fuel Process. Technol.* **2009**, *90*, 525–530. [[CrossRef](#)]
34. Martín-Alfonso, M.; Partal, P.; Navarro, F.; García-Morales, M.; Gallegos, C. Use of a MDI-functionalized reactive polymer for the manufacture of modified bitumen with enhanced properties for roofing applications. *Eur. Polym. J.* **2008**, *44*, 1451–1461. [[CrossRef](#)]
35. Zhao, P.Z.; Wang, Y.S.; Zhu, J.H.; Wen, Q.Z. Effect of heat treatment on the microphase separation behavior of polyurethane. *Spec. Purp. Rubber Prod.* **2007**, *28*, 20–28. (In Chinese) [[CrossRef](#)]

Disclaimer/Publisher’s Note: The statements, opinions and data contained in all publications are solely those of the individual author(s) and contributor(s) and not of MDPI and/or the editor(s). MDPI and/or the editor(s) disclaim responsibility for any injury to people or property resulting from any ideas, methods, instructions or products referred to in the content.